RSC Advances

Isomorphous substitution of Cr by Fe in MIL-101 framework and its application as a novel heterogeneous photo-Fenton catalyst for reactive dyes degradation

Journal:	*RSC Advances*
Manuscript ID:	RA-ART-07-2014-006522.R1
Article Type:	Paper
Date Submitted by the Author:	19-Aug-2014
Complete List of Authors:	Vu, Tuan; Institute of Chemistry - VAST, Surface Chemistry Le, Giang; Institute of Chemistry - VAST, Surface Chemistry Dao, Canh; Institute of Chemistry - VAST, Surface Chemistry Dang, Lan; College of education-Hue university, Nguyen, Kien; Institute of Chemistry - VAST, Surface Chemistry Dang, Phuong; Institute of Chemistry - VAST, Surface Chemistry Tran, Hoa; Institute of Chemistry - VAST, Surface Chemistry Duong, Quang; Hue University of Education, Van Nguyen, Tuyen; Vietnam Academy of Science and Technology, Lee, Gun; Pukyung National University,

SCHOLARONE™
Manuscripts

Isomorphous substitution of Cr by Fe in MIL-101 framework and its application as a novel heterogeneous photo-Fenton catalyst for reactive dyes degradation

Tuan.A.Vu[1*], Giang.H.Le[1], Canh.D.Dao[1], Lan.Q.Dang[2], Kien.T.Nguyen[1], Phuong.T.Dang[1], Hoa.T.K.Tran[1], Quang.T.Duong[3], Tuyen.V.Nguyen[1] and Gun.D.Lee[4]

[1]Institute of Chemistry, Vietnam Academy of Science and Technology (VAST), 18 Hoang Quoc Viet, Cau Giay District, Hanoi, Vietnam

[2]College of education-Hue university, Vietnam, [3]Hue University of Education, Vietnam

[4]College of Engineering, Pukyong National University, 113, Engineering Building 4, Yongdang Campus, Busan, South Korea

Corresponding author: vuanhtuan.vast@gmail.com

Abstract

Partial isomorphous substitution of Cr by Fe in MIL-101 framework was succeeded by direct synthesis using hydrothemal method (conventionally, solvothermal method). The products were characterized by XRD, EDX, N_2 adsorption (BET), TEM, UV-vis, FTIR, XPS and testing Photo-Fenton activities in the degradation of commercial reactive dyer RR195. From FTIR and XPS results, it revealed that Fe is really incoporated into MIL-101 framework. From EDX result,amount of ca.25% of Cr atoms in MIL-101 framework is substituted by Fe atoms. Fe substituted Cr-MIL-101 showed high adsorption capacity of reactive dye. Moreover, this material exhibited high Photo-Fenton activity in reactive dye degradation, opening the new application of MOFs as a novel heterogenous Photo-Fenton catalyst.

Keywords: Isomorphous substitution, MOFs, Photo-Fenton catalyst, Reactive Dyes.

I – Introduction

Metal-Organic Frameworks (MOFs) are a new class of hybrid materials assembled with metal cation and organic linker, have received a great attention in recent years due to their unique properties: high surface area, crystalline open structures, tunable pore size, functionality and their application in separation, gas storage, adsorption and catalysis [1-8]. Some of the most interesting properties of MOFs are inherently linked with the secondary building units (SBUs) coordination sphere. Coordinatively unsaturated metal sites can interact with lewis-base guests through coordination bonds. Because of their site isolation, some SBUs feature metal cations with up to four open coordination site, priming them for inner-sphere redox reactivity [9]. Therefore, metal substitution can alter directly the SBUs, creating the new properties of the material by introducing various metal centres in the same framework, one may cumulate different catalytically active

sites and/or tune adsorptive, optoelectronic, magnetic properties [10-14]. Recently, Brozek et al [2] succeded to substitute metal nodes (Ti^{3+}, $V^{2+/3+}$, $Cr^{2+/3+}$, Mn^{2+}, Fe^{2+}) in MOF-5 by post-synthetic ion methasis. They provided the first evidence of redox reactivity in MOF-5 analogues with single electron oxidation of Cr^{2+} MOF-5 and demonstrated that Fe-MOF-5 actives NO via electron transfer from Fe center. Khan et al [3] investigated the effect of central metal ions of analogues-BDCs on the adsorptive removal of benzothiophene (BT) among Cr^{3+}, Al^{3+} and V^{3+} substituted BDCs loaded by $CuCl_2$, V-BDCs exhibited much higher BT adsorption capacity (5-10 times) as compared to that of Cr-BDC and Al-BDC. They claimed that V^{3+} was oxidized by Cu^{2+} resulting V^{4+} and Cu^{1+} which favored the interaction (π-complexation) between Cu^{+} in the $CuCl_2$/V-BDC and BT. Koh et al [15] calculated the CO_2 adsorption enthalpies of 36 metal-substituted (M=Be, Mg, Ca, Sr, Sc, Ti, V, Cr, Mn, Fe, Co, Ni, Cu, Zn, Mo, W, Sn and Pb) M-DOBCD and M-HKUST-1 by computationally thermodynamic screening, they identified 13 compounds having ΔH values within the targeted thermodynamic window $-40 \leq \Delta H \leq -75$ kJ/mol (M=Mg, Ca, Sr, Sc, Ti, V, Mo, W on M-DODBC and M=Be, Mg, Ca, Sr, and Sc on M-HKUST-1). This result is very helpful in guiding and predicting synthesis of metal substituted MOFs used as selective adsorbents for CO_2 capture. Until recently, a serious short coming of MOFs that limited their application in adsorption and catalysis due to their low thermal and and hydrolytic stability. Férey and Co-worker[16] reported the discovery of the mesoporous Cr-MIL-101 which showed high resistance to water, common solvents and temperature (up to 320^{o}C). Attempts to incorporate metals into MIL-101 frameworks have been made. Szilágui et al [17] claimed that they succeeded to substitute Al and Fe in Cr-MIL-101 frameworks by post-synthetic cation exchange. The proof for metal (Fe) substitution was based on the result obtained from Mőssbauer spectroscopy. Recently, Alcaniz et al [18] developed a new consecutive post-functionalization method for metals incorporation into Cr-MIL-101 framework by using oxamate as chelating agent. By this route, highly dispersed Pd and Au nanoparticles can be incorporated into Cr-MIL-101 framework and these materials showed high selectivity and activity in Suzuki-Miyaura condensation and benzyl alcohol oxidation. A novel composite incorporating a trivacant Keggin ($[A\text{-}PW_9O_{34}]^{9-}$, PW_9) into Cr-MIL-101 through an impregnation method was developed by Granadeiro et al [19]. This composite exhibited high effeciency in monoterpene oxidation and oxidative desulfurization of fuel oil.

In the present work, we report the incorporation of Fe into Cr-MIL-101 by direct synthesis using hydrothermal method (conventionally, solvothermal method), characterization of Fe- Cr-MIL-101 by XRD, EDX, N_2 adsorption (BET), TEM, UV-vis, FTIR, XPS and its use as a heterogeneous Photo-Fenton catalyst for photo-catalytic

degradation of commercial reactive dyer RR195. To our best knowledge, this is the first work reporting the stable Fe-substituted MIL-101 by hydrothermal treatment and its application a novel heterogeneous photo-Fenton catalyst.

II- Experimental section

Synthesis of Cr-MIL-101 and Fe-Cr-MIL-101

Synthesis of Cr-MIL-101 was carried out by dissolving 8mL of 5M HF in 192 mL of H_2O and 6.56g of terephthalic acid (H_2BDC), then to this mixture, 16g of $Cr(NO_3)_3 \bullet 9H_2O$ was added and stirred for 3h. The mixture was put into a teflon lined autoclave and heated in an oven at 220^oC for 9 h. The solid product was filtered through Whatman filter paper, dried and put into a teflon bottle containing 95% ethanol and heated in an oven for 22h at 100^oC. The product was filtered, washed with hot EtOH and dried at 100^oC for 3 - 4h.

Fe-Cr-MIL-101 was synthesized using the similar procedure for Cr-MIL-101 synthesis except that amount of 25% wt. Cr was replaced by Fe. Attempts to increase amounts of Fe for obtaining higher Fe subtitution was not succeeded. Thus, instead of Fe-Cr-MIL-101, Fe-BDC was formed.

Characterization

The powder X-ray diffraction (XRD) patterns of the samples were recorded on a Shimadzu XRD-6100 analyzer with Cu K_α radiation (l=1.5417Å). High resolution transmission electron microscopy (HR-TEM) using JEOL 1010 instrument operating at 80 kV with magnification of 25,000–100,000 was used to obtain HR-TEM photograps of the samples. The X-ray photoelectron spectroscopy (XPS) measurement was performed on the ESCALab MKII spectrometer using Mg K_α radiation. The FT-IR spectra of the samples were measured by the KBr pellet method (BIO-RAD FTS-3000). EDX of samples were measured using JEOL JSM 6500F spectrometer.

Photo-Fenton reaction

Pyrex glass bottles of 50 ml solution containing reactive dye RR195 (conc. of 100ppm), MIL-101 catalysts (conc. of 300 mg/L) and H_2O_2 (conc. of 136 mg/L) were used as batch reactors. Solar irradiation was simulated using UV-A range lamps (4 lamps, power of 15w for each lamp). The emission spectrum between 400 and 800 nm follows the solar spectrum. Photo-Fenton reaction of dye RR195 was carried out under stirring condition, at room temperature and pH of 5.5. The samples were collected at diffirent reaction time.

Concentrations of RR195 were determined by using a Lambda 35 UV-vis spectrophotometer intensities of the band at 540 nm.

III - Results and Discussion

X-ray Diffraction (XRD)

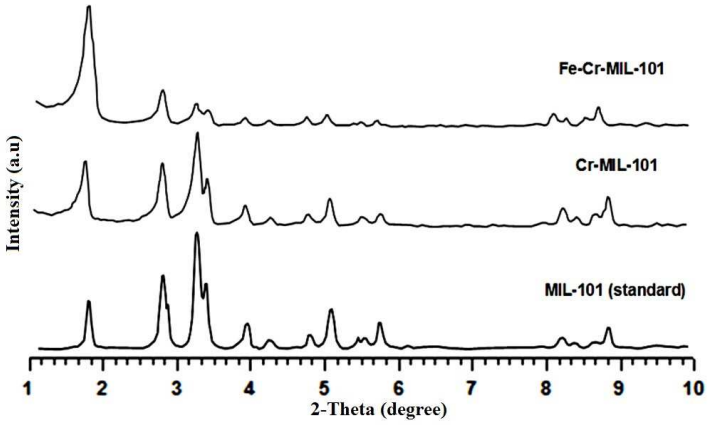

Fig. 1. XRD patterns of Fe-Cr-MIL-101 and Cr-MIL-101 and MIL-101 (standard)

The XRD patterns of Cr-MIL-101 and Fe- Cr-MIL-101 are plotted in Fig.1. In patterns of both samples, the main diffraction peaks appear at 2θ of 1.8, 2.8, 3.2, 3.9, 5.1, 8.2 and 8.8 are identical to those reported for MIL-101[16]. Both Cr-MIL-101 and Fe- Cr-MIL-101 patterns showed the flat background and high intensities, indicating high crystallinity of the samples. In the case of Fe- Cr-MIL-101, no Fe_2O_3 and other phases were detected, indicating high purity of the sample.

Energy-dispersive X-ray spectroscopy (EDX)

Chemical compositions of Cr-MIL-101 and Fe- Cr-MIL-101 are given in table 1. As seen in table 1, the Cr-MIL-101 contained 63% C atoms, 30.8% O atoms and 5.6% Cr atoms while the Fe- Cr-MIL-101 contained 63% C atoms, 31% O atoms, 4.2% Cr atoms and 1.4% Fe atoms, respectively. It was observed that both samples contained almost the same amounts of C and O, they distinguished only by amounts of Cr and Fe. In the case of Fe- Cr-MIL-101, the amount of ca.25% Cr atoms was substituted by Fe atoms.

Table 1. Chemical compositions of Cr-MIL-101 and Fe- Cr-MIL-101

Sample	C % mass	O % mass	Cr % mass	Fe % mass	C % atoms	O % atoms	Cr % atoms	Fe % atoms
Fe-Cr-MIL 101	48.81	32.37	13.9	4.93	63.08	31.4	4.15	1.37
	48.85	34.41	12.14	4.45	62.23	32.91	3.57	1.22
	48.62	30.19	15.66	5.53	63.89	29.79	4.75	1.56
Average	**48.76**	**32.323**	**13.9**	**4.97**	**63.067**	**31.367**	**4.1567**	**1.3833**
Cr-MIL 101	49.29	31.88	17.77	-	63.39	30.78	5.28	-
	48.41	30.35	20.81	-	63.56	29.92	6.31	-
	48.63	33.05	17.93	-	62.56	31.92	5.33	-
Average	**48.78**	**31.76**	**18.84**	**-**	**63.17**	**30.87**	**5.64**	**-**

Scanning Electron Microscope (SEM) and Transmission Electron Microscopy (TEM)

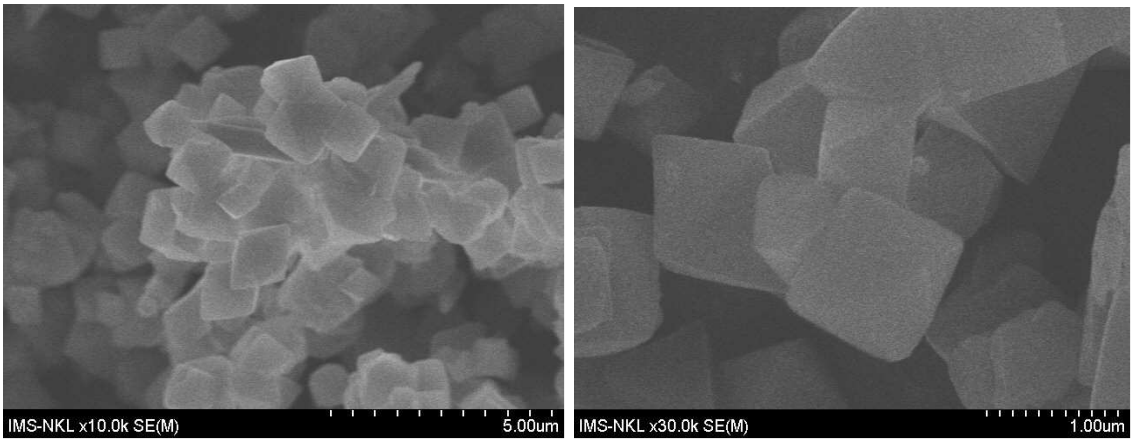

Fig.2. SEM photographs of Cr-MIL-101 and Fe- Cr-MIL-101

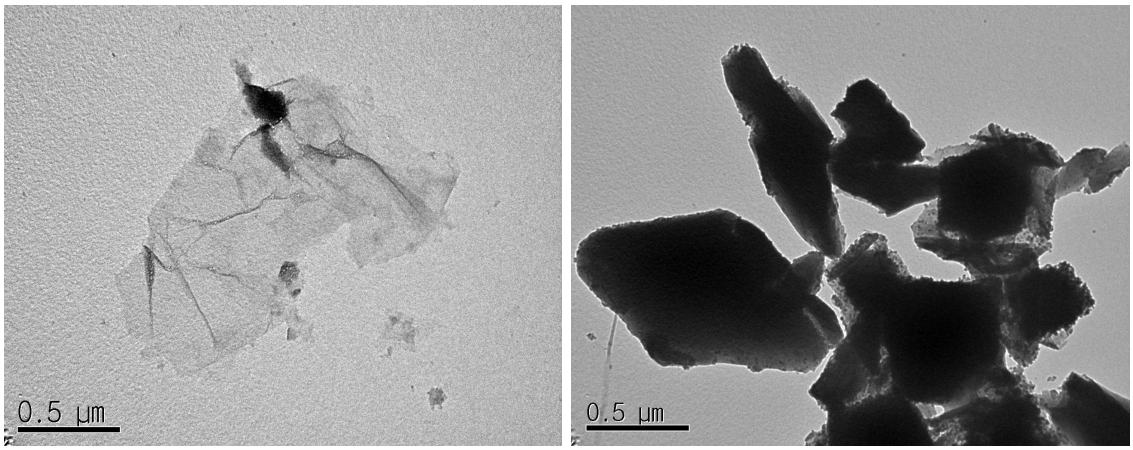

Fig.3. TEM photographs of Cr-MIL-101 and Fe-Cr-MIL-101

SEM photographs of Cr-MIL-101 and Fe-Cr-MIL-101 samples are presented in Fig.2. both samples have the cubic shape with the crystal size of 0.9-1.0 μm. the distribution of crystal size is uniform.

TEM photographs of Cr-MIL-101 and Fe-Cr-MIL-101 are illustrated in Fig.3. The cubic crystals of both samples as seen in SEM photographs were broken in smaller crystals with different shape and size. Thus, MIL-101 is extremely sensitive to the electron beam and in usual condition, the structure collapses under the electron beam exposure [20]. In the case of Fe-Cr-MIL-101, irons were well dispersed within crystals as indicated by uniform and intense dark color.

N_2 adsorption / desorption (BET)

The nitrogen adsorption/desorption isotherms of Cr-MIL-101 and Fe-Cr-MIL-101 are plotted in Fig.4. The adsorption isotherms showed three distinct adsorption steps. At a very low relative pressure of 0.01-0.15, the uptake increased very fast. This step is assigned to the filling of micropores of MIL-101. Between the relative pressure of 0.15-0.25, the slope of the adsorption isotherm decreased. This second step is related to the filling of small mesopores. The third step taken place at the relative pressure of 0.25-0.8 corresponded to the final pore filling. The overall course of the adsorption isotherm is characteristic as reported for MIL-101 structure [21].

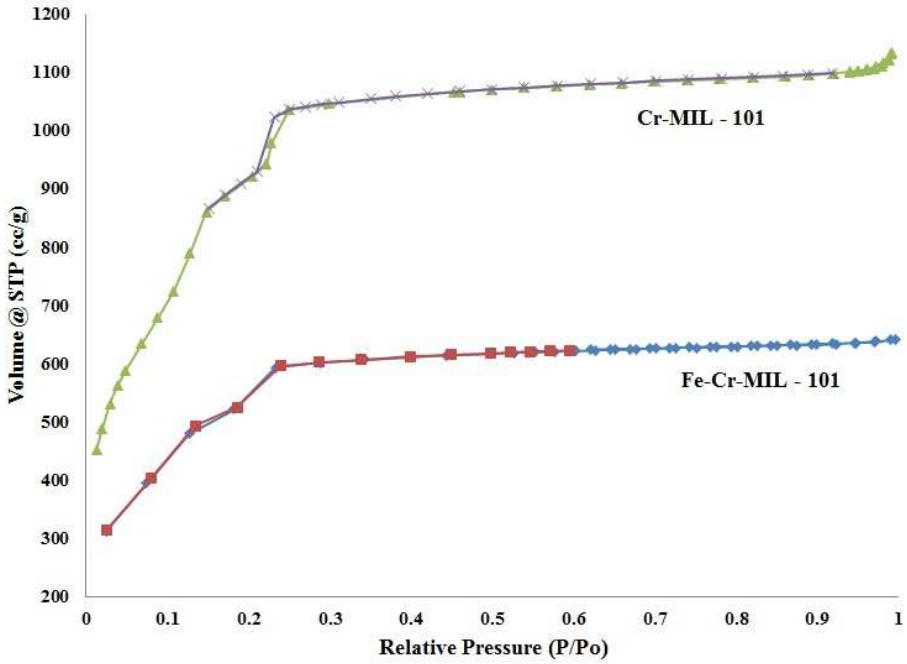

Fig.4. The nitrogen adsorption/desorption isotherms of Cr-MIL-101 and Fe- Cr-MIL-101

Table 2. Textual characteristics of Cr-MIL-101 and Fe- Cr-MIL-101

Samples	S_{BET} (m^2/g)	Total pore volume (cm^3/g)	Average pore size (nm)
Cr-MIL 101	3532	1.7526	1.99
Fe-Cr-MIL 101	2997	0.9958	2.01

Textual characteristics of Cr-MIL-101 and Fe-Cr-MIL-101 are given in table 2. In comparison to Cr-MIL-101, Fe- Cr-MIL-101 had smaller surface area ($2997 m^2/g$) and pore volume ($0.99 cm^3/g$)

Fourier Transform Infrared Spectroscopy (FTIR)

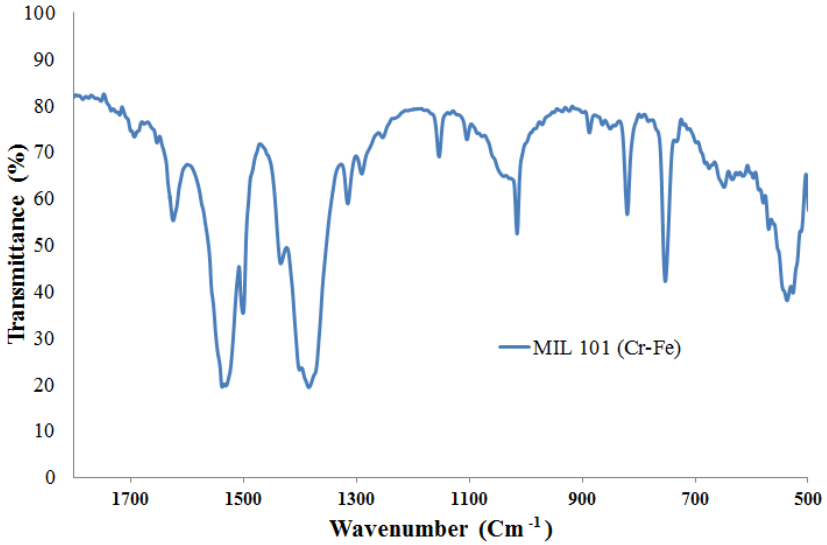

Fig.5. FTIR spectrum of Fe-Cr MIL-101

Figure 5 presented the FTIR spectrum of Fe-Cr MIL-101. In the sekectal region of 500-1700 cm^{-1}. Strong bands in the region of 1750-1300 cm^{-1} correspond to ν_{as} (COO), ν_s(COO) and ν (C-C) vibrations, implying the presence of dicarboxylate linker in MIL-101 framework [22]. Rather weak band at 1117 and sharp band at 749 cm^{-1} are attributed to σ(C-H) and γ(C-H) vibrations of aromatic rings, respectively. The band at 1635 cm^{-1} is assigned to the vibration of C=O group. The intense peak at $540cm^{-1}$ is related to the Fe-O vibration while Cr-O vibration in Cr-MIL-101 framework appear at 577 cm^{-1} [23]. This result proves the Fe incorporation into Cr-MIL-101 framework.

X-ray photoelectron spectroscopy (XPS)

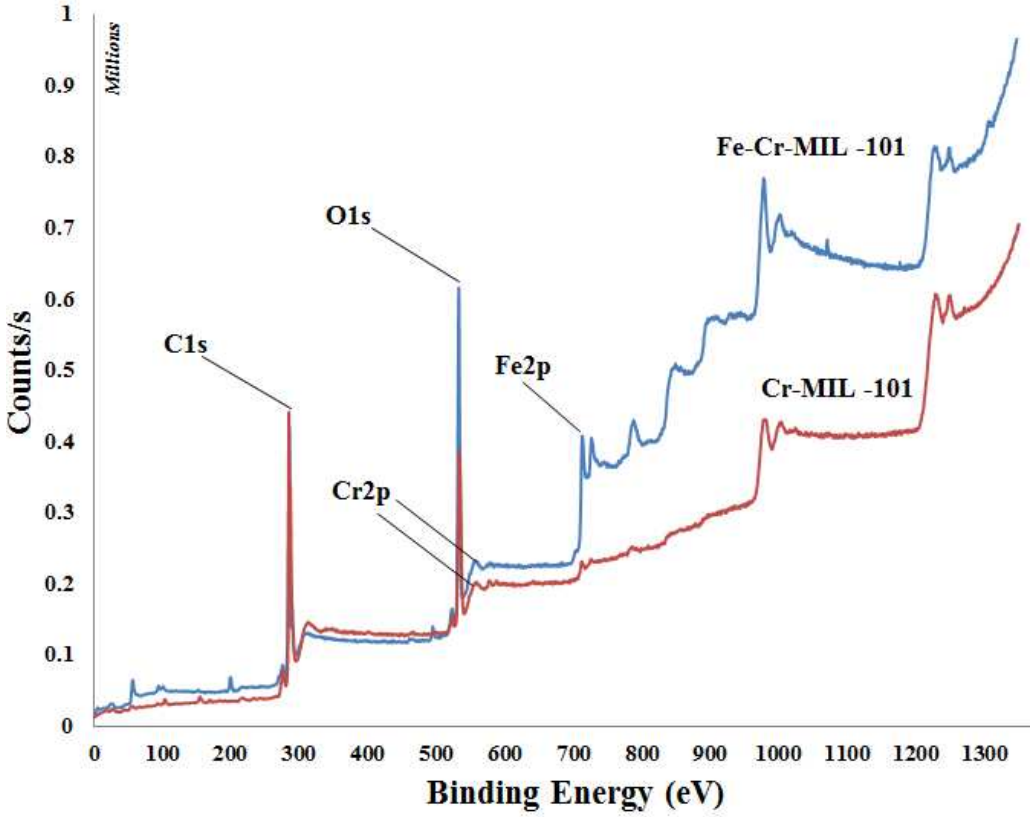

Fig. 6. XPS spectra of Fe-Cr-MIL 101 and Cr-MIL 101

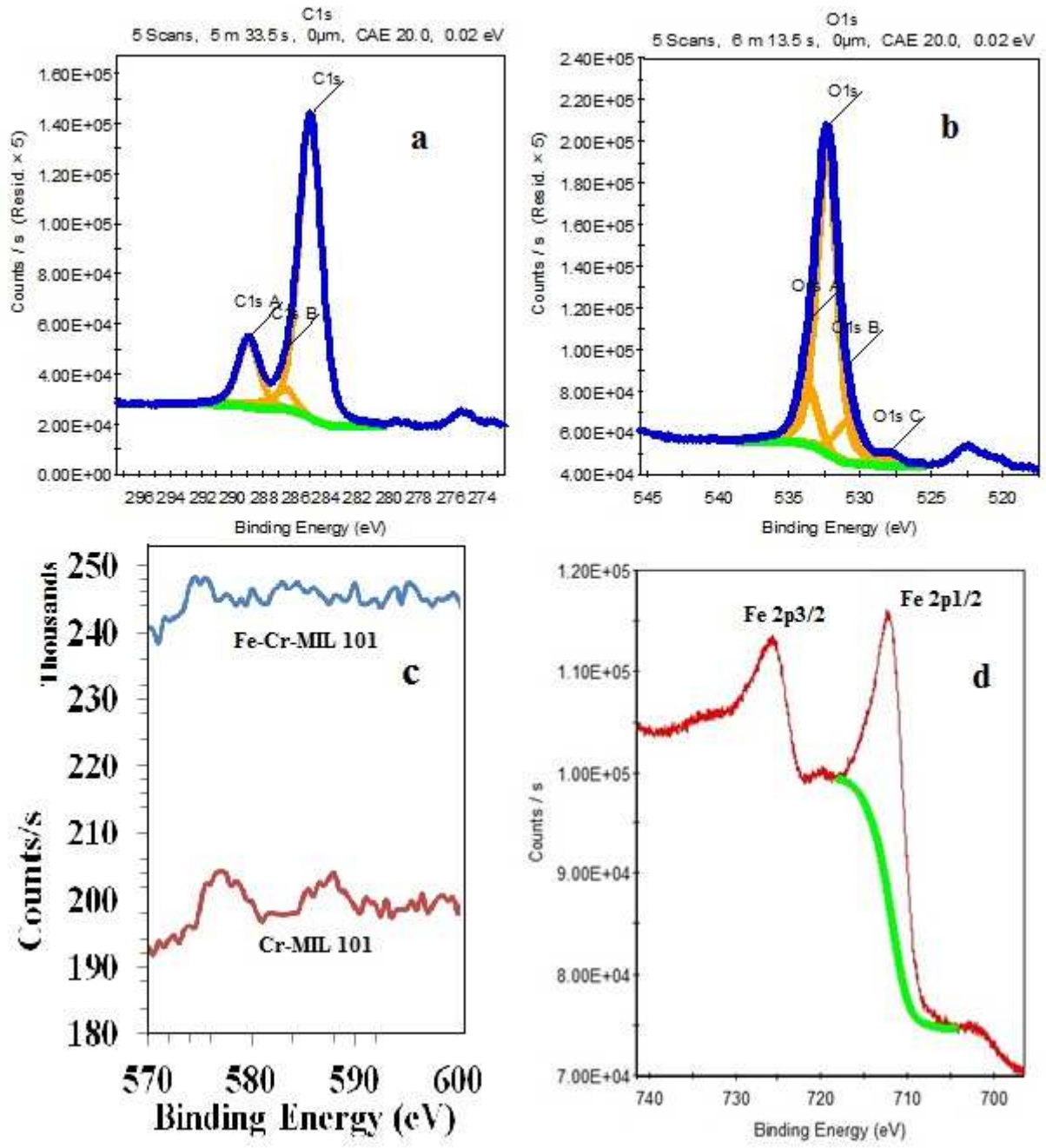

Fig.7. C1s, O1s, Cr2p and Fe2p spectral lines in the XPS spectrum of Cr-Fe MIL 101

XPS spectra of Cr-MIL-101 and Fe- Cr-MIL-101 are shown in Fig.6. As expected, Cr-MIL-101 sample contained the three elements C,O and Cr whereas Fe-Cr MIL-101 contained the four elements C, O, Cr and Fe. The XPS spectrum of C1s for Fe-Cr MIL-101 (Fig.7a) showed two peaks at 284.9 and 288.7 eV, corresponding to phenyl and carboxyl signals, respectively [24-26]. In the XPS spectrum of O1s (Fig.7b), the O1s peak at 531.7 and 533.1 eV related to the Fe-O-C species [27]. Figure 6c presented the

XPS spectra of Cr2p for Cr-MIL-101 and Fe-Cr-MIL-101 samples. The spectrum of Cr2p for Cr-MIL-101 showed two peaks at 576.8 and 585.5 eV corresponding to the $Cr2p_{1/2}$ and $Cr2p_{3/2}$ signals, repectively [29]. In the case of Fe-Cr-MIL-101, these signal intensities were much diminished, indicating that a large amount of Cr was replaced by Fe(Fig.7c).

In the Fe 2p spectrum for Fe-Cr-MIL-101 (Fig.7d) appeared two peaks at 711.9 and 725.7 eV which corresponding to Fe2p3/2 and Fe 2p1/2 signals [28]. This result is in agreement with that reported for Fe-BTC [26]. Baln et al [30] investigated the Fe_2O_3 deposited MIL-101 and reported that the Fe2p3/2 and Fe2p1/2 signal appeared at 710.0 and 723.9 eV, respectively. From the XPS result, it can be concuded that Fe is really incorporated into MIL-101 framework.

Adsorption and photo-Fenton catalysts

The dye effluents from textile industries are significant sources in environmental pollution. Fenton and Photoassisted Fenton technologies as the important advanced oxidation process (AOPs) have been widely applied in textile waste water treatments. In recent years, the active heterogeneous Fenton catalysis is gradually replacing the homogeneous system by immobilized Fe ions on the polymer substrates [31]. Fe substituted MOFs used as heterogeneous Photo-Fenton catalysts in degradation of reactive dyes have not yet been reported. Therefore, in this study we examine the Fenton and photo-Fenton catalytic activities of Fe- Cr-MIL-101 in degradation of reactive red dye 195 (RR195). Reactive red dye 195 is a commercial product which is often used in the textile dyeing process. This dye is very stable and difficult to be degraded. The structure is presented as below.

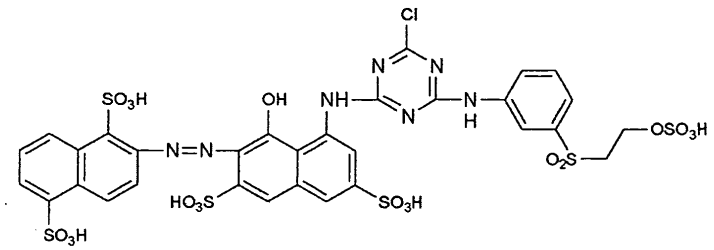

C.I. Reactive Red 195

The changes of RR195 concentrations in aqueous solution by adsorption and Fenton reation over Cr-MIL-101 and Fe- Cr-MIL-101 are plotted in Fig. 8. As seen in Fig 8, both Cr-MIL-101 and Fe-Cr-MIL-101 showed high adsorption rate and capacity. After one hour of adsorption (in dark), concentrations of RR195 decreased to the value of 35-45%

as compared to the initial concentration (Co). Note that here we used relatively low adsorbent concentration (0.3g adsorbent/L solution) as compared to the common use (1.0g adsorbent/L solution) in the research works reported in the literature. In comparison to Cr-MIL-101, was observed on Fe-Cr-MIL-101 higher RR195 adsorption capacity. Normally, it is expected that adsorption capacity of Fe-Cr-MIL-101 should be lower due to its lower surface area (2997m^2/g for Fe-Cr-MIL-101 and 3532m^2/g for Cr-MIL-101). The higher adsorption capacity of Fe-Cr-MIL-101 could be explained by its higher affinity to form the Fe-Azo dye complex [32]. There was only a few paper reported dyes adsorption onto MIL-101. Haque et al [33] claimed that Cr-MIL-101 exhibited the excellent adsorption capacity of methyl orange. Chen et al [34] investigated the adsorption ability of reactive dye XO (xylenol orange) onto Cr-MIL-101 and found that Cr-MIL-101 showed much higher XO adsorption capacity as compared to that of traditional adsorbents like MCM-41 and activated carbons.

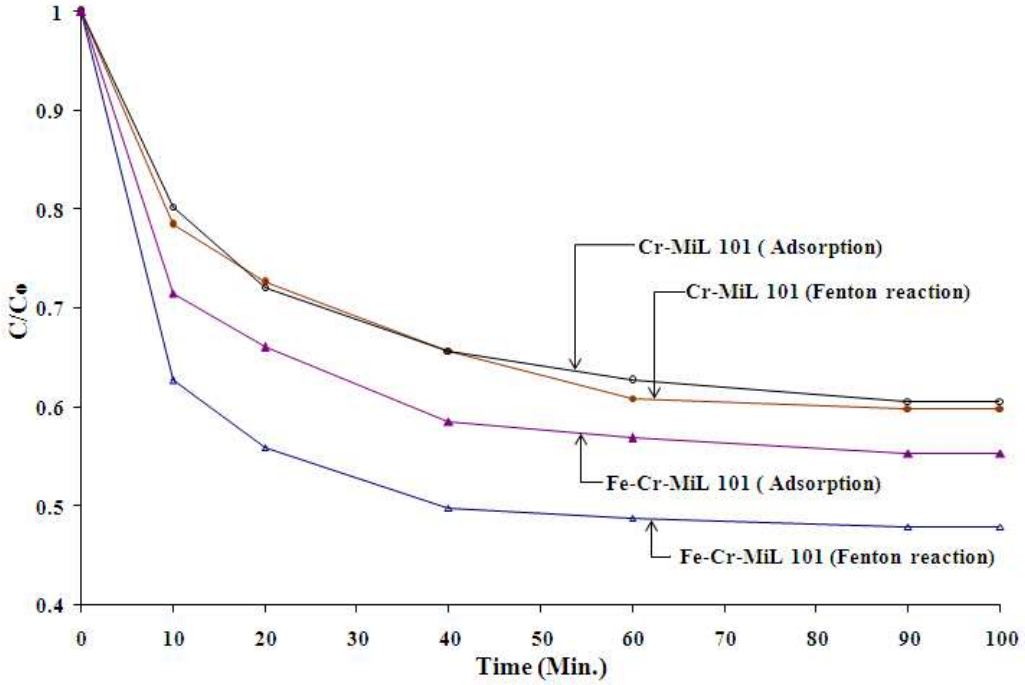

Fig. 8. Changes of RR195 concentrations as function of time over Fe-Cr-MIL 101 and Cr-MIL 101

To test the Fenton catalytic activities of Cr-MIL-101 and Fe-Cr-MIL-101, oxidation of reactive dye RR195 solution (100ppm) in presence of H_2O_2 was carried out . As seen in Fig.8, Cr-MIL-101 exhibited almost no Fenton catalytic activities since no changes in the Fenton reaction and adsorption curves were noted.

In the case of Fe- Cr-MIL-101, low Fenton catalytic activity (ca.10%) conversion was observed. To evaluate the Photo-Fenton catalytic activities of Cr-MIL-101 and Fe-Cr-MIL-101, oxidation of reactive dye RR195 solution (100ppm) in presence of H_2O_2 under visible light irradiation (simulated sun light) was performed. The changes of RR195 concentrations on reaction time are plotted in Fig.9 and Fig.10.

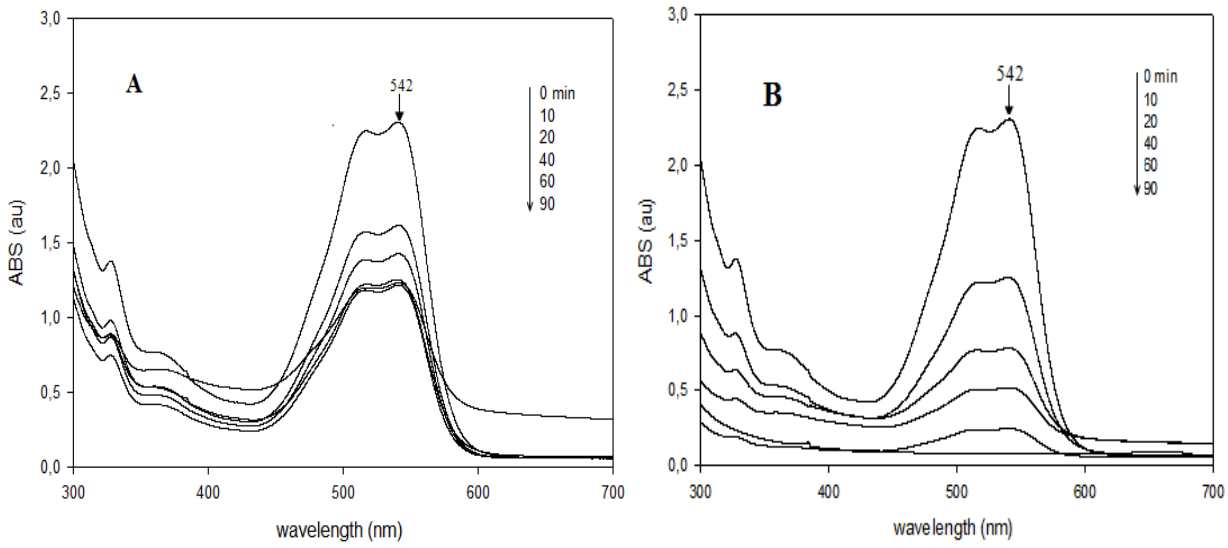

Fig. 9. UV-Vis spectra of RR 195 at different reaction time over Cr-MIL 101(A) and Fe-Cr-MIL 101 (B)

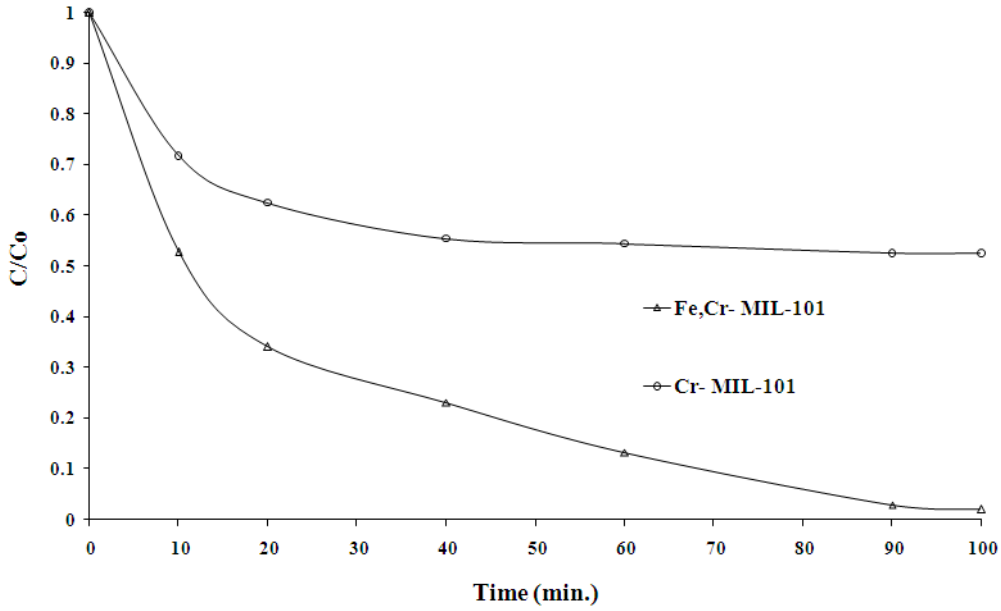

Fig. 10. Changes of RR195 concentrations as function of reaction time over Fe-Cr-MIL 101 and Cr-MIL 101

As observed in Fig.10, Cr-MIL 101 did not show photo-Fenton catalytic activity (compare Fig.8 and Fig.10) whereas Fe-Cr-MIL 101 exhibited high photo-Fenton catalytic activity. Thus, after 100 minutes reaction under visible light irradiation, the RR195 conversion reached to the value of 98%. In comparison to the Fenton reaction in dark, the RR195 conversion reached the value of ca.50%,only. This clearly indicated that the activation of H_2O_2 by Fe-Cr-MIL-101 to produce more amounts of •OH radicals, thus greatly enhancing the degradation efficiency of RR195. In the presence of H_2O_2, the positive synergistic effects could contribute to the catalytic performance of Fe-Cr-MIL-101. Fe(III) on the surface of Fe-Cr-MIL-101 can catalyze the decomposition of H_2O_2 to produce •OH radicals by the Fenton-like reaction [35-37].

$$\text{Fe(III)species} + H_2O_2 \rightarrow \text{Fe(II)species} + HO_2^{\bullet} + H^+ \quad (1)$$

$$\text{Fe(II)species} + H_2O_2 \rightarrow \text{Fe(III)species} + \bullet OH + OH^- \quad (2)$$

On the other hand, H_2O_2 as an efficient scavenger could capture the photoinduced electrons in the excited Fe-Cr-MIL-101 to form •OH radicals (Eqs. (3) and (4)).

$$\text{Fe-Cr-MIL-101} + h\nu \rightarrow h^+ + e^- \quad (3)$$

$$H_2O_2 + e^-_{\text{(Fe-Cr-MIL-101)}} \rightarrow \bullet OH + OH^- \quad (4)$$

To investigate more deeply the photocatalytic degradation of reactive dye RR195, some important effect such as pH, initial concentration of RR195 and stability of photocatalyst Fe-Cr MiL 101 have been evaluated.

The effect of initial pH on the degradation efficiency of RR195 over Fe-Cr MiL 101/simulated solar/H_2O_2 system was determined. As shown in Fig. 11, the Fe-Cr MiL 101 catalyst exhibited high photocatalytic activity at low value pH of 3.2 -5.5. At higher pH of 7, the photocatalytic activity decreased considerably, especially at pH of 10, photocatalytic activity was very low. This observation is consistent with the other catalytic systems of organometallic coordination polymers reported previously that Fenton reaction usually performed at acidic condition.

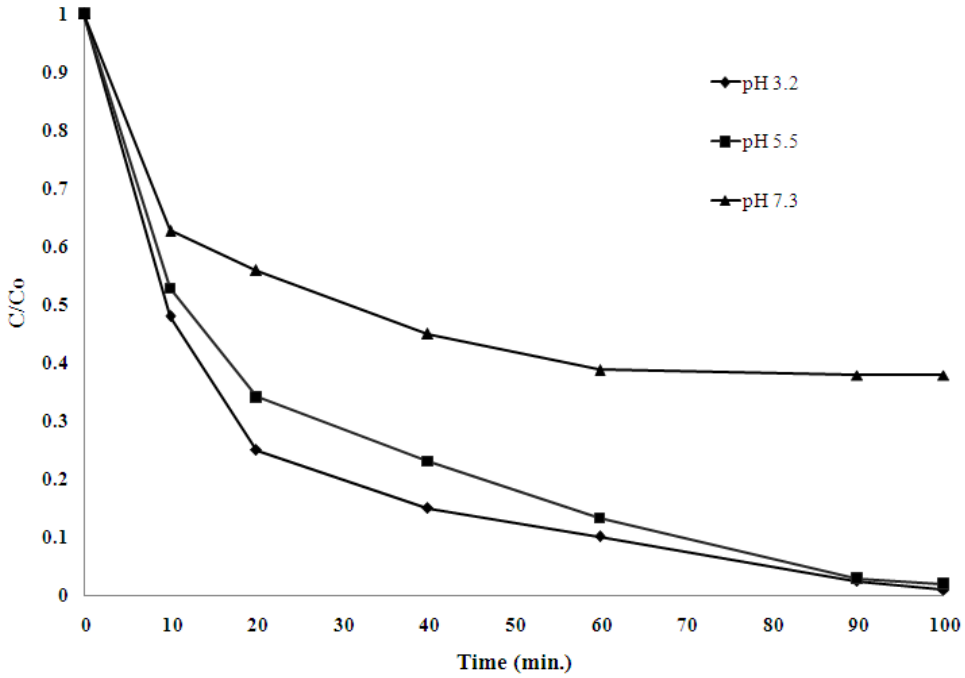

Fig.11 Effect of initial pH on RR195 degradation over Fe-Cr-MiL-101 under simulated solar irradiation

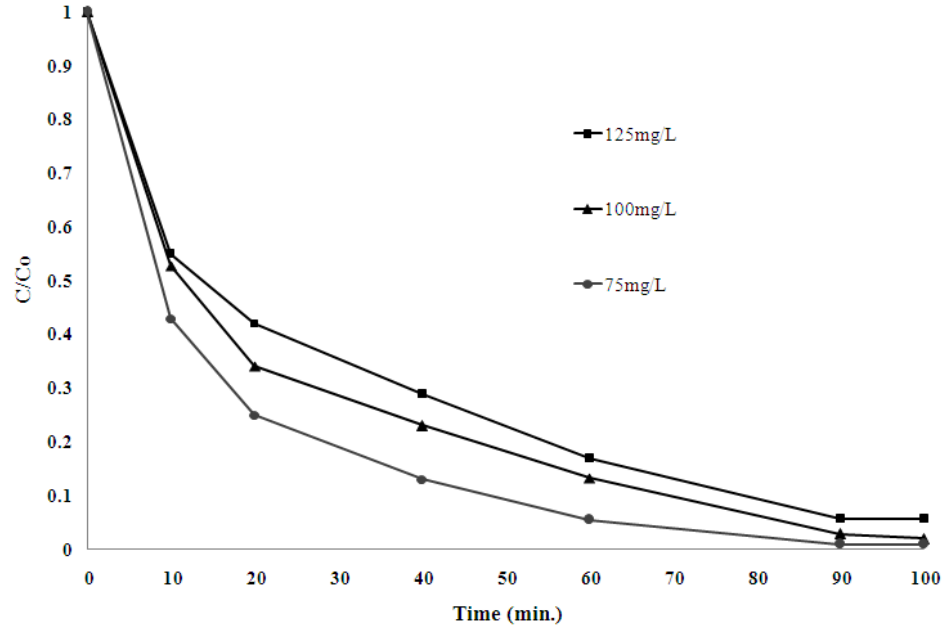

Fig.12 Effect of initial RR195 concentration on degradation over Fe-Cr-MiL-101 under simulated solar irradiation

The influence of initial dye concentration on the degradation of RR195 over Fe-Cr-MiL-101/simulated solar/H_2O_2 system was also evaluated. As seen in Fig.12, the

degradation efficiency of RR195 strongly depend on the initial dye concentration. Thus, with increasing initial dye concentration, photocatalytic activity decreased considerably.

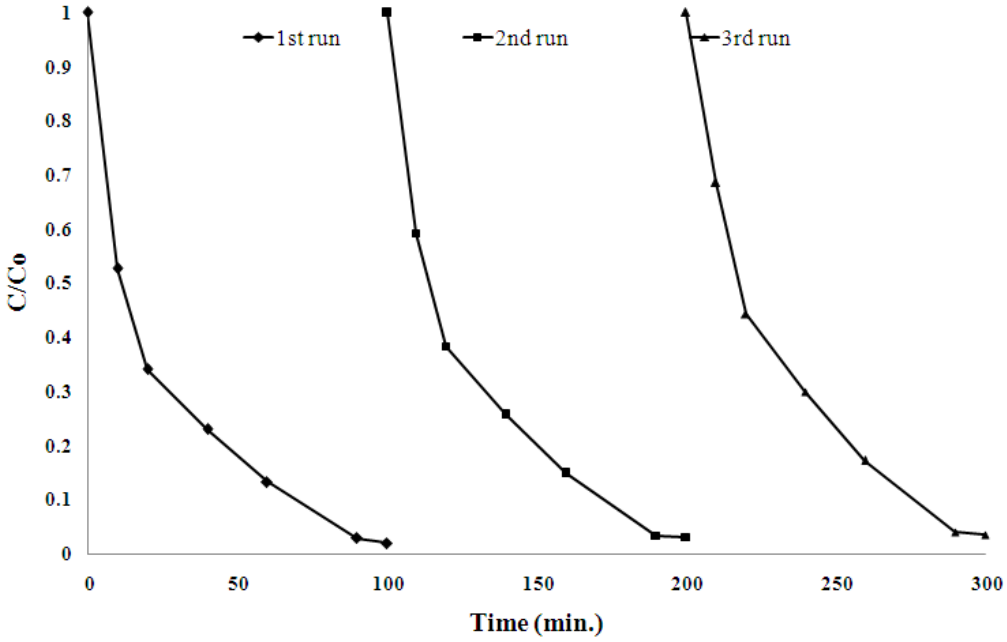

Fig.13 The cycling runs of RR195 degradation over Fe-Cr-MiL-101 under simulated solar irradiation

The recyclability of Fe-Cr-MiL-101 was examined by circulating runs in the catalytic degradation of RR195 over Fe-Cr-MiL-101/simulated solar/H_2O_2 system, the results presented in Fig.13. As observed in Fig.13, photocatalytic performance of the Fe-Cr-MiL-101 catalyst remained almost unchanged after three recycles, indicating that Fe-Cr-MiL-101 catalyst is very stable and can be reused. Moreover, the high stability of Fe-Cr-MiL-101 was confirmed by iron leaching measurements (determed by AAS). After 30, 60 and 90 minutes of reaction, iron leaching was 0.1, 0.3 and 1.5 ppm . This results indicated that iron leaching is negligible. This also is consitent with that reported for Fe -MiL-101 [38].

Conclusion

From the obtained results, some conclusions can be drawn:

- Partial isomorphous substitution of Cr by Fe in MIL-101 framework was succeeded by direct synthesis using hydrothemal method.

- From FTIR and XPS results, it revealed that Fe is really incorporated into MIL-101 framework. From EDX result, amount of ca.25% of Cr atoms in MIL-101 framework is substituted by Fe atoms.
- Fe-Cr-MIL-101 showed high adsorption capacity of reactive dye RR195. Moreover, this material exhibited high Photo-Fenton activity and high stability in reactive dye degradation, opening the new application of MOFs as a novel heterogenous Photo-Fenton catalyst.

Acknowledgments

The authors thanks the National Foundation for Science and Technology Development of Vietnam—NAFOSTED **(Grant no. 104.05-2013.64)** for financial support.

References

[1]. O.V. Zalomaeva, K.A. Kovalenko, Y.A. Chesalov, M. S. Mel'gunov, V.I. Zaikovskii, V.V. Kaichev, A. B. Sorokin, O.A. Kholdeeva and V.P. Fedin, Dalton Trans., 2011,40, 1441-1444.

[2]. C. K. Brozek and M.Dinca, J. Am. Chem. Soc. 2013, 135, 12886−12891.

[3]. N. A.Khan, S. H. Jhung, Journal of Hazardous Materials, 2013, 260, 15, 1050–1056.

[4] T.R. Cook, Y.-R. Zheng, P.J. Stang, Chem. Rev. 2013, 113, 734–777.

[5] S.T. Meek, J.A. Greathouse, M.D. Allendorf, Adv. Mater. 2011, 23,249–267.

[6] H. Wu, Q. Gong, D.H. Olson, J. Li, Chem. Rev. 2012, 112, 836–868.

[7] J.-R. Li, J. Sculley, H.-C. Zhou, Chem. Rev. 2012, 112, 869–932.

[8] P. Horcajada, R. Gref, T. Baati, P.K. Allan, G. Maurin, P. Couvreur, G. Férey, R.E. Morris, C. Serre, Chem. Rev. 2012, 112, 1232–1268.

[9]. Dincă M, Dailly A, Liu Y, Brown CM, Neumann DA, Long JR. J Am Chem Soc. 2006 ;128 (51):16876-83.

[10]A. Dhakshinamoorthy, M. Alvaro and H. Garcia, Chem. Commun., 2012,48, 11275-11288.

[11] A. Phan, Alexander U. Czaja, F. Gándara, C. B. Knobler and O. M. Yaghi, Inorg. Chem., 2011, 50 (16), 7388–7390.

[12] Bloch E.D, Murray L.J, Queen W.L, Chavan S, Maximoff S.N, Bigi J.P, Krishna R, Peterson V.K, Grandjean F, Long G.J, Smit B, Bordiga S, Brown C.M, Long J.R, J Am Chem Soc. 2011 133 (37):14814-22.

[13] Y. Fu, D. Sun, Y. Chen, R. Huang, Dr. Z. Ding, X. Fu, Z. Li, .Angew. Chem., Int. Ed.2012, 51, 3364−3367.

[14] C. K. Brozek and M. Dinc, Chem. Sci.2012, 3, 2110−2113.

[15]. Koh H.S, Rana M.K, Hwang J, Siegel D.J. Phys Chem Chem Phys. 2013, 15(13):4573-81.

[16]. G. Férey, C. Mellot-Draznieks, C. Serre, F. Millange, J. Dutour, S. Surblé, I. Margiolaki, Science 23 September 2005: 309, 5743, 2040-2042.

[17]. P.Á. Szilágyi, P.Serra-Crespo, I. Dugulan, J. Gascon, H. Geerlingsad and B. Dam, Cryst. Eng. Comm, 2013, 15, 10175-10178.

[18]. J. Juan-Alcañiz, J.Ferrando-Soria, I. Luz, P. Serra-Crespo, E.Skupien, V.P. Santos, E. Pardo, F. X. Llabrés i Xamena, F.Kapteijn, J. Gascon, Journal of Catalysis , 2013, 307, 295–304.

[19]. Carlos M. Granadeiro, André D. S. Barbosa, S. Ribeiro, I. C. M. S. Santos, B.de Castro, L.Cunha-Silva and S. S. Balula, Catal. Sci. Technol., 2014,4, 1416-1425.

[20]. O. I. Lebedev, F. Millange, C. Serre, G. Van Tendeloo, and G. Férey, Chem. Mater., 2005, 17 (26), 6525–6527.

[21]. D.Y. Hong, Y. K. Hwang, C. Serre, G. Férey and J.S. Chang, Advanced Functional Materials, 19, 10, 2009, 1537–1552.

[22] D.W. Brown, A.J. Floyd, M. Sainsbury, Willey, New York, 1988.

[23]. R.Fazaeli, H. Aliyanb, M. Moghadam, M.Masoudinia, Journal of Molecular Catalysis A: Chemical, 2013, 374–375, 46–52.

[24] Gardella J.A., S.A. Ferguson and R.L. Chin, Applied Spectroscopy, 1986. 40(2): 224-232

[25]. L. J. Gerenser, J. Vac. Sci. Technol. A 1990,8, 3682.

[26]. B.J. Zhu, X.Y. Yu, Y. Jia, F.M. Peng, B. Sun, M.Y. Zhang, T. Luo, J.H. Liu, and X.J. Huang, J. Phys. Chem. C, 2012, 116 (15), 8601–8607.

(27) Srivastava, S.; Badrinarayanan, S.; Mukhedkar, A. J.Polyhedron 1985, 4, 409.

(28) Yamashita, T.; Hayes, P.Appl. Surf. Sci.2008, 254, 2441-2449.

[29]. T. V. Vu, H. Kosslick, A. Schulza, J. Harloff, E. Paetzold, M. Schneider, J. Radnik, N.Steinfeldt, G. Fulda, U. Kragl, Applied Catalysis A: General, 2013, 468, 410–417.

[30]. A. M. Balu, C. S. Ki Lin, H. Liu, Y.Li, C. Vargas, R. Luque, Applied Catalysis A: General, 2013, 455, 261–266.

[31] B.Li, Y. Dong, Z. Ding, Y. Xu, and C.Zou, International Journal of Photoenergy, 2013 Article ID 169493,10 pages.

[32]. A. R. Rahmani, M. Zarrabi, M. R. Samarghandi, A. Afkhami, H. R. Ghaffari, Iranian Journal of Chemical Engineering 2010, 7, 1.

[33] E. Haque, J.E. Lee, I.T. Jang, Y.K. Hwang, J.S. Chang, J. Jegal, S.H. Jhung, J. Hazard. Mater. 2010, 181, 535–542

[34]. C. Chen, M. Zhang, Q. Guan, W. Li, Chemical Engineering Journal, 2012, 183, 60–67.

[35]. Q. Chen, P. Wu, Z.Dang, N. Zhu, P. Li, J. Wu, X. Wang, Separation and Purification Technology, 2010, 71, 3, 315–323.

[36]. Lunhong Ai, Caihong Zhang, Lili Li, Jing Jiang, Applied Catalysis B: Environmental 148–149 (2014) 191–200.

[37]. Wen-Tao Xu,Lin Ma,Fei Ke,Fu-Min Peng,Geng-Sheng Xu,Yu-Hua Shen,Jun-Fa Zhu,Ling-Guang Qiu and Yu-Peng Yuan, Dalton Trans., 2014, 43, 3792 –3798.

[38]. Nataliya V. Maksimchuk,Olga V. Zalomaeva,Igor Y. Skobelev, Konstantin A. Kovalenko,Vladimir P. Fedin and Oxana A. Kholdeeva, Proc. R. Soc. A 8 July 2012 vol. 468 no. 2143 2017-2034.